Supporting online material for

Ultracompact silicon/polymer laser with an absorption-insensitive nanophotonic resonator

Thilo Stöferle,[1] Nikolaj Moll,[1] Thorsten Wahlbrink,[2] Jens Bolten,[2] Thomas Mollenhauer,[2] Ullrich Scherf,[3] Rainer F. Mahrt[1]*

[1]IBM Research – Zurich, Säumerstrasse 4, CH-8803 Rüschlikon, Switzerland. [2]Advanced Microelectronic Center Aachen (AMICA) AMO GmbH, Otto-Blumenthal Strasse 25, D-52074 Aachen, Germany. [3]Macromolecular Chemistry Group and Institute for Polymer Technology, Bergische Universität Wuppertal, Gauss-Strasse 20, D-42119 Wuppertal, Germany.

*To whom correspondence should be addressed. E-mail: tof@zurich.ibm.com

1. Materials and Methods

1.1. Photonic Simulations

Full 3D Finite-Difference Time-Domain (FDTD) simulations were performed, which calculate the temporal behavior and therefore the actual propagation of the electromagnetic waves in the structure[1]. To obtain the absorption spectra, a calculation cell of size $24a \times 1a \times 17a$ was used with periodic boundary conditions in the grating direction. The lattice constant a is discretized by 24 mesh points. The absorption of Si and dispersion of MeLPPP are implemented by employing material dispersion of the form of one harmonic resonance in the plasmon pole model. The grating structure is excited by a plane wave with surface-normal propagation exhibiting a temporal Gaussian envelope and a broad spectral width. For single gratings, the reflectivity spectrum is calculated from the optical fluxes. For cavities, the resonance frequencies and quality factors are calculated by harmonic inversion.

1.2. Fabrication

The laser devices are fabricated on silicon-on-insulator (SOI) substrates consisting of a 2-µm-thick buried oxide layer and a 340-nm-thick Si device layer. The structures are defined by electron-beam lithography with 100 keV beam energy using hydrogen silsesquioxane (HSQ) as negative tone resist. Pattern transfer is achieved in a two-step HBr-chemistry-based inductively coupled reactive-ion etch process[2]. The entire process flow is optimized to maintain the dimensional accuracy of the cylindrical columns of the grating structures. Methyl-substituted ladder-type poly(p-phenylene) (MeLPPP; M_n = 31500, M_w = 79000) was synthesized as described elsewhere[3]. MeLPPP is dissolved in

toluene and spin-coated over the grating structures. The film thickness of approximately 700 nm is measured with a profilometer (Dektak, Veeco) and spectroscopic ellipsometry (VASE, Woollam).

1.3. Characterization

The excitation light at λ = 440 nm is provided from a white-light optical parametric amplifier (TOPAS-C, Light Conversion) pumped by a regenerative amplifier (Legend Elite, Coherent), which is seeded with a mode-locked Ti:Sapphire laser (Tsunami with Millennia pump laser, Spectra-Physics). The pulse duration is 100 – 200 fs, with a repetition rate of 1 kHz. Residual excitation light at longer wavelengths is removed by a short-pass filter. The pump pulse is focused onto the sample in a home-built confocal microscope setup through an objective with f = 2 mm and NA = 0.5 (100X M Plan Apo NIR, Mitutoyo). All measurements are performed at room temperature. To prevent photo-oxidation the samples are kept in vacuum during the measurement. The light emitted from the laser is collected through the same objective, and any reflected or scattered pump light at λ < 460 nm is removed by a long-pass filter. For the time-integrated measurements, the light is guided through a multi-mode fiber to a high-resolution spectrograph (500 mm Acton Spectra Pro, Princeton Instruments, with gratings of 300 lines/mm and 1800 lines/mm) and detected with a liquid-N_2-cooled charge-coupled device (CCD) (Spec-10, Princeton Instruments). For the time-resolved measurements, the light is coupled directly into a spectrograph (300 mm Acton Spectra Pro, Princeton Instruments, with 150 lines/mm grating) and recorded with a streak camera system (C5680, Hamamatsu).

2. Modeling

2.1. HCG reflectivity at inclined incidence

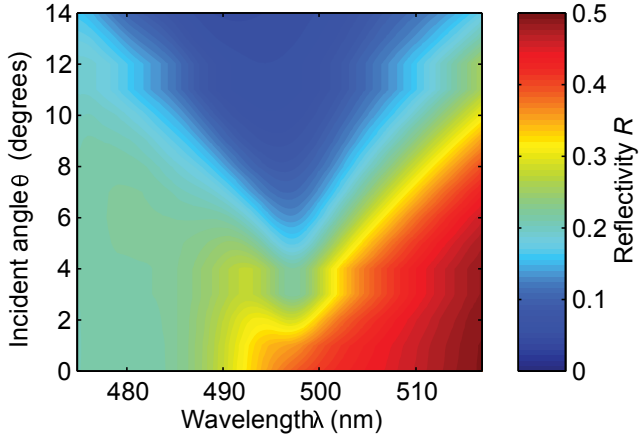

Figure S1. Reflectivity spectrum of the HCG as a function of incident angle (3D FDTD simulations). For increasingly inclined incidence, the maximum of the reflectivity shifts to longer wavelengths which is characteristic for a diffractive reflection mechanism. In contrast, for photonic band gap reflectors, the peak reflectivity would shift to shorter wavelengths.

2.2. Rate equation analysis

For modeling the laser emission we use a rate equation approach for microcavity semiconductor lasers[4,5]. In this model, the photon number in the lasing mode is given by:

$$S = \frac{1}{2}\left[U + \left(V^2 + \frac{4\xi(\beta - 1)}{A\tau_s} P + \frac{4\xi}{A\tau_s}(1-\xi) \right)^{1/2} \right]$$

with

$$U = P - 1 - \left(\frac{1}{A\tau_s} - 1 \right)\xi$$

$$V = U + \frac{2\xi}{A\tau_s}$$

Here $(1 - \xi)$ denotes the fraction of spontaneous emission which is lost from the cavity, A is the free space spontaneous emission rate, τ_s is the exciton lifetime, and β is the fraction of the spontaneous emission coupled into the cavity mode. The pump energy $P=f\,p$ is proportional to the incident energy p, whereas the detected emission is $I(p) = a\,S(p) + b\,p$. The latter term accounts for additional luminescence which is proportional to the pump power, because we detect not only the cavity radiation but also scattered photoluminescence. We fix the parameters to the following values: $\xi = 0.48$ (vertical guiding due to total internal reflection), $A = 1/10$ ps (from streak camera measurements), and $\tau_s = 10$ ps (from streak camera measurements). The scaling factors f, a and b and the parameter β are fitted to the data (see Fig. 3b in the manuscript). The fitted value of $\beta = 3 \times 10^{-4}$ indicates that the device does not operate in the Purcell-enhanced regime, which is consistent with the streak camera measurements (Fig. 4f in the manuscript).

3. Further optical characterization

3.1. Polarization

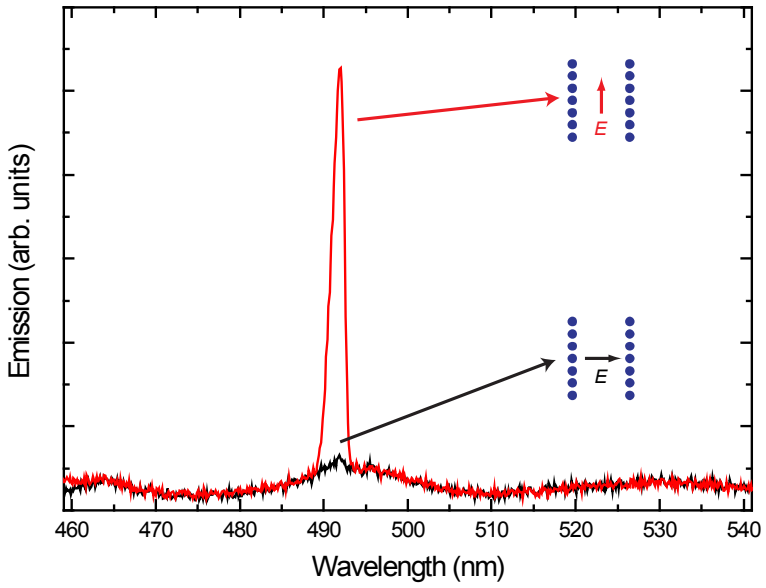

Figure S2. Polarized laser output. When the device is pumped above threshold, the light of the emitted laser pulses is polarized. The graph shows the emission spectrum for different orientations of a sheet polarization analyzer (extinction ratio 6000:1) in front of the fiber guiding the light to the spectrometer. While the broad luminescence from the polymer appears unpolarized, the laser peak is only observed when the polarization axis of the analyzer is set parallel to the grating lines. This confirms the expectation from the FDTD simulation in which a TE-like resonant mode is observed.

3.2. Line width

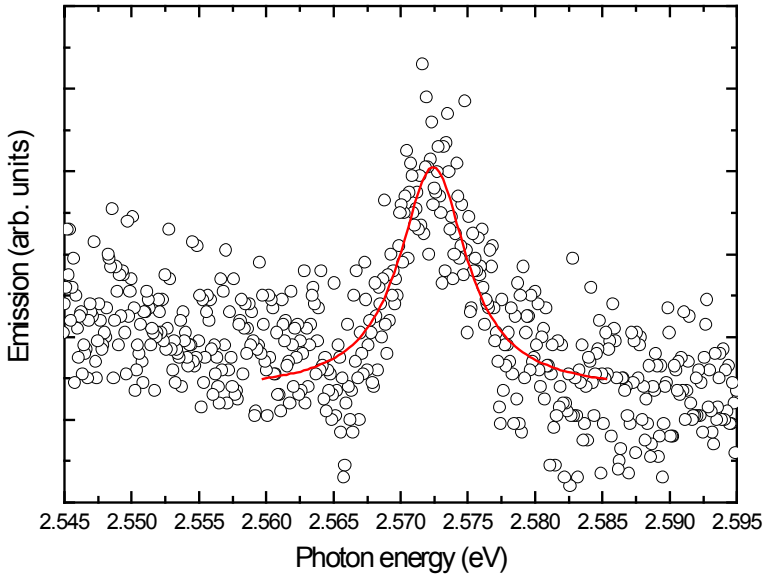

Figure S3. Laser line width. The laser emission is studied with a high-resolution spectrograph (grating with 1800 lines/mm and 0.5 m length). From a Lorenz fit (red line) we find that the laser peak has a full width at half maximum of 6 meV, corresponding to $\Delta\lambda \approx 1$ nm in wavelength.

3.3. *Multimode lasing*

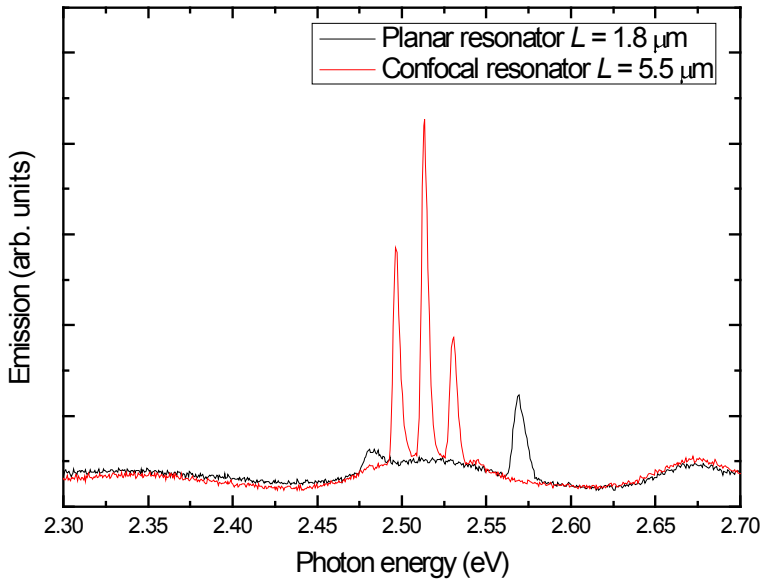

Figure S4. Multimode lasing. Several types of resonators are investigated to demonstrate the versatility of the concept. In general, the free spectral range of the cavity decreases for increasing resonator length. The emission spectrum above the threshold of a device with a planar Fabry-Pérot-type resonator of 1.8 μm length is shown (black line). The wavelength separation of the two resonant peaks is ~88 meV. For comparison, a confocal-like resonator of 5.5 μm length (mirror curvature radius = distance) is shown (red line), where the spectral separation between the peaks is ~17 meV.

4. References

(1) A. F. Oskooi *et al.*, *Computer Phys. Comm.* **181**, 687-702 (2010).

(2) T. Wahlbrink *et al.*, *Microelectronic Engineering* **78**, 212-217 (2005).

(3) U. Scherf, A. Bohnen, K. Müllen, *Die Makromolekulare Chemie* **193**, 1127-1133 (1992).

(4) H. Yokoyama, S.D. Brorson, *J. Appl. Phys.* **66**, 4801 (1989).

(5) K. A. Shore, M. Ogura, *Optical and Quantum Electronics* **24**, 209 (1992).